PLOS PATHOGENS

RESEARCH ARTICLE

The fungal expel of 5-fluorocytosine derived fluoropyrimidines mitigates its antifungal activity and generates a cytotoxic environment

Luis Enrique Sastré-Velásquez[1], Alex Dallemulle[1], Alexander Kühbacher[1], Clara Baldin[1], Laura Alcazar-Fuoli[2,3], Anna Niedrig[4], Christoph Müller[4], Fabio Gsaller[1]*

1 Institute of Molecular Biology, Biocenter, Medical University of Innsbruck, Innsbruck, Austria, **2** Mycology Reference Laboratory, National Centre for Microbiology, Instituto de Salud Carlos III (ISCIII), Madrid, Spain, **3** Center for Biomedical Research in Network in Infectious Diseases (CIBERINFEC-CB21/13/00105), Instituto de Salud Carlos III, Madrid, Spain, **4** Department of Pharmacy, Center for Drug Research, Ludwig-Maximilians University of Munich, Munich, Germany

* fabio.gsaller@i-med.ac.at

Citation: Sastré-Velásquez LE, Dallemulle A, Kühbacher A, Baldin C, Alcazar-Fuoli L, Niedrig A, et al. (2022) The fungal expel of 5-fluorocytosine derived fluoropyrimidines mitigates its antifungal activity and generates a cytotoxic environment. PLoS Pathog 18(12): e1011066. https://doi.org/10.1371/journal.ppat.1011066

Editor: Joshua J. Obar, Dartmouth College, Geisel School of Medicine, UNITED STATES

Received: August 25, 2022

Accepted: December 14, 2022

Published: December 27, 2022

Data Availability Statement: All relevant data are within the manuscript and its Supporting Information files.

Funding: This research was funded by the Austrian Science Fund (FWF), grant P31093 to F.G. and M2867 to C.B. The funders had no role in study design, data collection and analysis, decision to publish, or preparation of the manuscript.

Competing interests: The authors have declared that no competing interests exist.

Abstract

Invasive aspergillosis remains one of the most devastating fungal diseases and is predominantly linked to infections caused by the opportunistic human mold pathogen *Aspergillus fumigatus*. Major treatment regimens for the disease comprise the administration of antifungals belonging to the azole, polyene and echinocandin drug class. The prodrug 5-fluorocytosine (5FC), which is the only representative of a fourth class, the nucleobase analogs, shows unsatisfactory *in vitro* activities and is barely used for the treatment of aspergillosis. The main route of 5FC activation in *A. fumigatus* comprises its deamination into 5-fluorouracil (5FU) by FcyA, which is followed by Uprt-mediated 5FU phosphoribosylation into 5-fluorouridine monophosphate (5FUMP). In this study, we characterized and examined the role of a metabolic bypass that generates this nucleotide *via* 5-fluorouridine (5FUR) through uridine phosphorylase and uridine kinase activities. Resistance profiling of mutants lacking distinct pyrimidine salvage activities suggested a minor contribution of the alternative route in 5FUMP formation. We further analyzed the contribution of drug efflux in 5FC tolerance and found that *A. fumigatus* cells exposed to 5FC reduce intracellular fluoropyrimidine levels through their export into the environment. This release, which was particularly high in mutants lacking Uprt, generates a toxic environment for cytosine deaminase lacking mutants as well as mammalian cells. Employing the broad-spectrum fungal efflux pump inhibitor clorgyline, we demonstrate synergistic properties of this compound in combination with 5FC, 5FU as well as 5FUR.

Author summary

Aspergillus fumigatus is the most common cause of invasive aspergillosis, a life-threatening fungal infection that is associated with worryingly high mortality rates. An antifungal

that is barely used for the treatment of aspergillosis illustrates the nucleobase analog 5-fluorocytosine (5FC). A major drawback of this antimycotic compound constitutes its low *in vitro* activity against *A. fumigatus*, which is owed to transcriptional repression of its uptake at neutral pH. In contrast to other clinically administered anti-*Aspergillus* agents, 5FC has no intrinsic antifungal capacity but has to be activated within the cell through the pyrimidine salvage pathway. In this work, we characterized a new set of pyrimidine salvage enzymes that participate in its metabolic activation and show that during 5FC exposure, *A. fumigatus* generates and exports significant amounts of its derived fluoropyrimidines such as cytotoxic 5-fluorouracil (5FU) and 5-fluorouridine (5FUR). This extrusion diminishes 5FC antifungal activity and, simultaneously, creates a toxic environment for mammalian cells, which suggests the use of fungal efflux pump inhibitors in combination with 5FC as a promising therapeutic strategy.

Introduction

Although several fungal species are able to cause life-threatening disease types, the highest death tolls are linked to infections by members of the genera *Aspergillus*, *Cryptococcus*, *Candida* and *Pneumocystis* [1, 2]. Among pathogenic *Aspergilli*, the major cause of life-threatening invasive aspergillosis remains the most prevalent mold pathogen *Aspergillus fumigatus* [3]. Being constantly exposed to its airborne spores, humans can inhale several hundred spores daily, which, due to their small size, are capable of entering the lung alveoli [4]. While the immune system in healthy individuals readily eliminates spores, their entrance in the lung is particularly dangerous for patients with a defective immune defense [4–6]. Widely employed treatment regimens against aspergillosis involve the use of azole, polyene or echinocandin antifungal agents [7, 8]. The nucleobase analog 5-fluorocytosine (5FC) is barely used to treat *Aspergillus*-induced diseases [7]. One obvious reason represents its negligible activity *in vitro*, however, previous work demonstrated a beneficial outcome of 5FC treatment on survival in murine infection models [9, 10]. In contrast to *Aspergillus*, 5FC shows potent activity against a variety of pathogenic species belonging to the genera *Candida* and *Cryptococcus*. For the treatment of infections caused by these pathogens, 5FC monotherapy is typically avoided due to rapid occurrence of resistance [11].

Most likely due to their apparent requirement for 5FC activity, common mechanisms of resistance in yeast and *A. fumigatus* are based on mutations in genes that impair its uptake (*FCY2*; *A. fumigatus fcyB*), cytosine deaminase (*FCY1*; *A. fumigatus fcyA*) and uracil phosphoribosyltransferase (*FUR1*; *A. fumigatus uprt*). While defective uptake and cytosine deaminase confer resistance specific to 5FC, mutations perturbing uracil phosphoribosyltransferase activity also lead to 5FU resistance [11, 12]. In addition to these, mutations leading to increased pyrimidine production as well as other genetic factors appear to play important roles in 5FC resistance [11]. In *Cryptococcus gattii*, for instance, mutations in the UDP-glucuronate decarboxylase (*UXS1*) gene increased 5FC resistance. Defects in the enzyme elevated glucuronic acid levels and led to changes in nucleotide metabolism [13]. In *Candida glabrata* an important role of aquaglyceroporins (*FPS1* and *FPS2*) in 5FC tolerance was suggested. Inactivating their gene function elevated 5FC intracellular accumulation, which resulted in increased 5FC susceptibility [14]. In *A. fumigatus*, a clear dependency of 5FC activity on the environmental pH has been demonstrated [9, 15]. At neutral pH, which is the common pH for antifungal susceptibility testing [16, 17], this mold displays intrinsic 5FC resistance, which was linked to

transcriptional repression of *fcyB*, coding for the main 5FC uptake protein [15]. At acidic pH, 5FC activity is significantly enhanced by upregulation of the gene [15].

In contrast to azoles, polyenes and echinocandins, 5FC *per se* is not toxic. For its activation, 5FC requires conversion into the nucleotide 5-fluorouridine monophosphate (5FUMP). Subsequent to its synthesis, 5FUMP is further metabolized into active 5-fluorinated ribo- and deoxyribo-nucleotides that hamper cell growth [11]. The main route of 5FUMP formation in fungi involves two enzymatic steps including 5FC deamination into 5FU by cytosine deaminase and phosphoribosylation thereof into 5FUMP *via* uracil phosphoribosyltransferase (**Fig 1A**) [11]. Compared to fungal species that are sensitive to 5FC, mammalian cells lack cytosine deaminase but possess two main routes of 5FUMP formation out of 5FU. 5FU can either be directly converted into 5FUMP by the *de novo* pyrimidine biosynthesis enzyme orotate phosphoribosyltransferase or indirectly *via* 5-fluorouridine (5FUR), which requires the consecutive action of uridine phosphorylase and uridine kinase [18].

Here, we characterized further pyrimidine salvage enzymes in *A*. *fumigatus* that participate in 5FC metabolic activation and demonstrate that, like mammalian cells, this mold harbors the enzymatic repertoire to generate 5FUMP indirectly. Measurements of extracellular 5FU and 5FUR during 5FC exposure indicated that *A*. *fumigatus* cells export both 5FC derivatives into the environment, which alleviates 5FC activity and, simultaneously, creates a toxic environment. Drug interaction analysis of 5FC, 5FU and 5FUR employing the fungal efflux pump inhibitor clorgyline (CLG) [19, 20] revealed synergistic properties with each pyrimidine analog and suggests that 5FC antifungal activity could be enhanced when used in combination with efflux pump inhibitors.

Results

Aspergillus fumigatus possesses pyrimidine salvage activities that mediate hydrolysis and phosphorylation of 5FUR

The pyrimidine salvage enzymes cytosine deaminase (FcyA, AFUB_005410) and uracil phosphoribosyltransferase (Uprt, AFUB_053020) are key enzymes in 5FC metabolic activation in *A*. *fumigatus*. While loss of FcyA (Δ*fcyA*) only confers hyper-resistance to 5FC, the absence of Uprt (Δ*uprt*) leads to high levels of resistance to 5FC and 5FU (≥100 μg/mL) [12]. In this work, resistance profiles of Δ*fcyA* and Δ*uprt* have been further assessed using 5FC and 5FU hyper doses and found that in the presence of 500 μg/mL 5FU, growth of Δ*uprt* was clearly inhibited (**Fig 1B**). This indicated the presence of further enzymes that are involved in 5FC metabolism.

Previous work in yeast demonstrated the presence of genes encoding pyrimidine salvage enzymes with uridine nucleosidase (Urh1p) and uridine kinase (Urk1p) activity with their main functions being the hydrolysis of uridine to uracil and the phosphorylation of uridine into uridine monophosphate, respectively [21]. BLASTP analysis using the respective *S*. *cerevisiae* protein sequences suggested the presence of a putative Urk1p ortholog, here named UrkA (AFUB_022460) as well as two Urh1p orthologs in *A*. *fumigatus*, here termed UrhA (AFUB_005870) and UrhB (AFUB_011230) (**Tables A and B in S1 Table**). To analyze the role of these genes in 5FUR/uridine metabolization, coding sequences of *urkA*, *urhA* and *urhB* were deleted in wild-type (wt). In addition, double deletion mutants Δ*urkA*Δ*urhA* and Δ*urkA*Δ*urhB* were generated, anticipating combined loss of 5FUR/uridine hydrolysis and phosphorylation activities. To further test that 5FUMP formation can only occur through Uprt or UrkA, the double deletion mutant Δ*uprt*Δ*urkA* was made. This mutant still encodes activities enabling the hydrolysis of 5FUR/uridine into 5FU/uracil and *vice versa*, however, the formation of 5FUMP/UMP should be blocked. The individual gene functions were analyzed

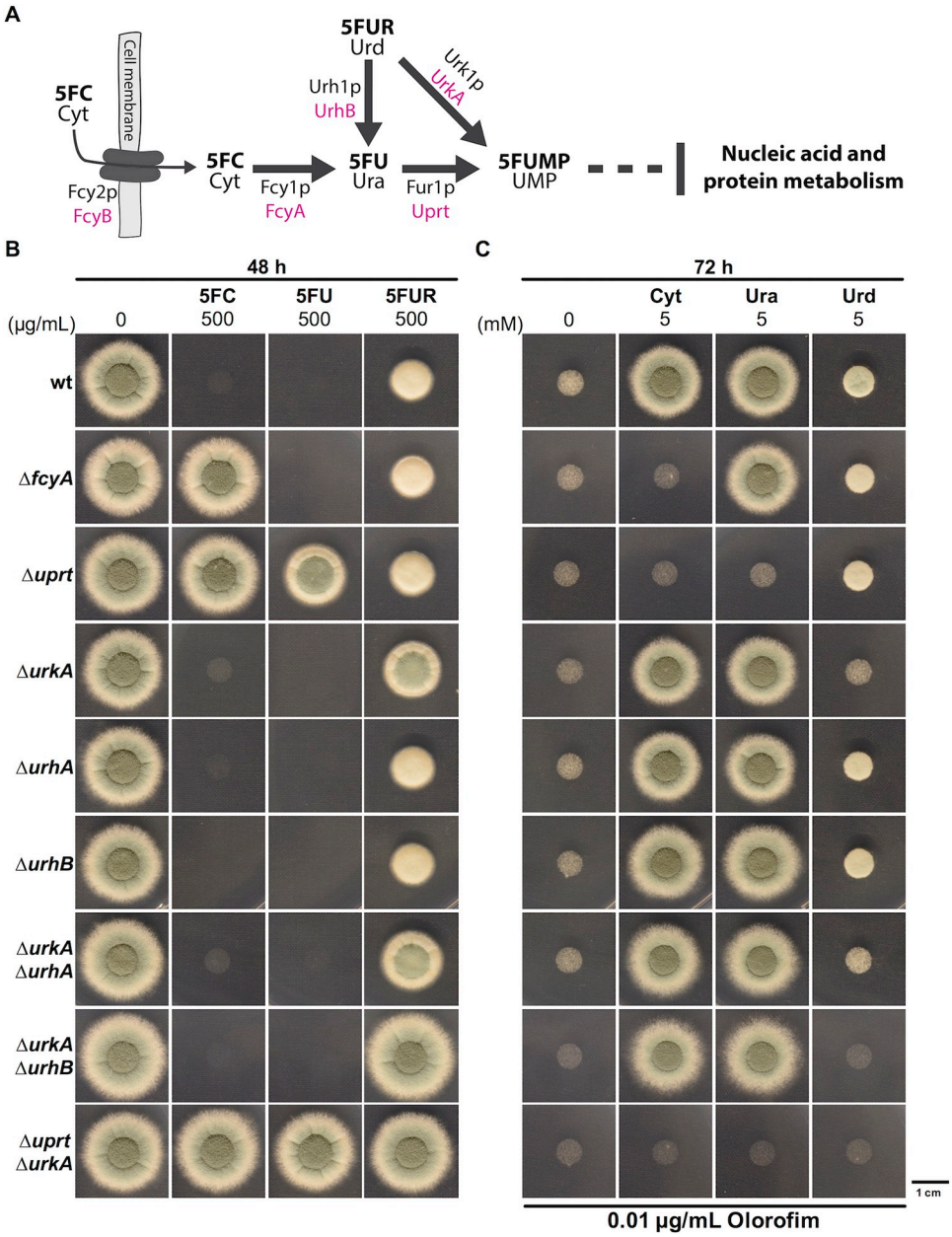

Fig 1. UrhB and UrkA mediate the hydrolysis and phosphorylation of 5FUR/uridine. **(A)** Scheme illustrating proteins involved in 5FC uptake and pyrimidine salvage pathway based metabolization of fluoropyrimidines in yeast (black) and *A. fumigatus* (magenta). **(B)** The role of uridine nucleosidase and uridine kinase encoding genes was determined by susceptibility testing. **(C)** Resistance analysis was complemented with a reversal assay studying the contribution of enzymes in the metabolization of nucleobases cytosine (Cyt) and uracil (Ura) as well as the nucleoside uridine (Urd) during *de novo* pyrimidine biosynthesis inhibition.

https://doi.org/10.1371/journal.ppat.1011066.g001

following two approaches. One included 5FC, 5FU and 5FUR resistance analysis of the different salvage pathway mutants. The second aimed to investigate the capacity of those strains to utilize cytosine, uracil and uridine for UMP generation during simultaneous inhibition of its *de novo* biosynthesis. In this case, the antifungal drug olorofim, inhibiting the essential enzyme dihydroorotate dehydrogenase [22], was supplemented to the medium.

Single mutants Δ*urhA* and Δ*urhB* showed wt-like susceptibility to 5FC, 5FU and 5FUR and growth of these strains could be promoted during olorofim treatment with either cytosine, uracil or uridine (Fig 1B and 1C). In agreement with the role of UrkA in the formation of 5FUMP/UMP out of 5FUR/uridine, Δ*urkA* displayed increased resistance to 5FUR and its growth could only marginally be recovered by uridine supplementation during *de novo* pyrimidine biosynthesis inhibition. This further indicates that 5FUR/uridine hydrolysis coupled to Uprt mediated 5FU/uracil phosphoribosylation is less efficient than the direct conversion of 5FUR/uridine into 5FUMP/UMP. Surprisingly, while Δ*urkA*Δ*urhA* with predicted block in 5FUR/uridine phosphorylation and hydrolyzation phenocopied the single deletion mutant Δ*urkA* with regard to its 5FUR resistance, Δ*urkA*Δ*urhB* displayed 5FUR hyper-resistance. By reintroducing a functional gene copy of *urhB* into Δ*urkA*Δ*urhB*, 5FUR resistance levels were restored, similar to that of Δ*urkA* (S1 Fig). This suggests that despite the higher identity of UrhA to yeast Urh1p (**Table A in** S1 Table), in *A*. *fumigatus* the hydrolysis of 5FUR/uridine is mainly mediated by UrhB. Δ*uprt*Δ*urkA* lacking both enzymes for direct 5FUMP/UMP generation, displayed hyper-resistance to 5FC, 5FU and 5FUR (Fig 1B) and its growth could not be promoted by the addition of cytosine, uracil or uridine to the growth medium (Fig 1C). Interestingly, despite the potential presence of salvage activities that enable the formation of 5FUMP/UMP independently of Uprt, growth of Δ*uprt* could not be recovered by cytosine or uracil during olorofim treatment. This, together with the high degree of 5FU resistance observed for Δ*uprt* compared to Δ*urkA*, suggests that 5FUMP/UMP synthesis occurs predominantly *via* Uprt.

Aspergillus fumigatus has the enzymatic capacity to convert 5FU into 5FUR

The growth impairment of Δ*uprt* at high concentrations of 5FU that can be overcome by the additional inactivation of *urkA* (Δ*uprt*Δ*urkA*) (Fig 1B), strongly suggests that *A*. *fumigatus* is able to convert 5FU into 5FUR. The catalytic cleavage of uridine into uracil by uridine nucleosidase (EC: 3.2.2.3) Urh1p, however, is anticipated to be irreversible [23]. Therefore, the enzyme that generates 5FUR out of 5FU in *A*. *fumigatus* still remained unclear. To rule out that *A*. *fumigatus* UrhA and/or UrhB might be involved in the conversion of 5FU into 5FUR, we first generated Δ*uprt*Δ*urhA* and Δ*uprt*Δ*urhB* double mutants and compared 5FU resistance to that of the recipient strain Δ*uprt*. Both double mutants showed the same level of 5FU resistance as their progenitor strain Δ*uprt* (Fig 2A), which suggested that the hydrolysis of 5FUR by uridine nucleosidase also occurs irreversible in *A*. *fumigatus*. In bacteria and mammals an enzyme termed uridine phosphorylase (EC: 2.4.2.3) catalyzes the reversible conversion of uridine into uracil [24, 25]. Only recently, two proteins with this enzymatic activity, PcUP1 and PcUP2, have been characterized in the plant pathogenic Oomycete *Phytophthora capsici* [26]. In the next step we looked for putative uridine phosphorylase orthologs using the corresponding *Escherichia coli* protein sequence Udp [27], mammalian UPP1 and UPP2 [28, 29] and that of PcUP1 and PcUP2. While BLASTP analyses did not reveal any putative orthologs, DELTA-BLAST suggested up to seven candidates, however with low overall identities (<21.9%). In addition to BLAST analyses, we searched the InterPro database [30, 31] for specific domains within Udp, UPP1, UPP2, PcUP1 and PcUP2 and found that all of them contained a nucleosidase phosphorylase domain, which was predicted in 10 proteins encoded by the genome of the *A*. *fumigatus* isolate A1163 (S2 Table). Noteworthy, this set of proteins included the ones identified by DELTA-BLAST. A1163 is part of the CEA10-lineage, the progenitor of A1160P+ which was used as wt reference in this work [32]. Two out of these proteins, which we termed UdpA (AFUB_097990) and UdpB (AFUB_047570), contained a predicted purine and uridine phosphorylase domain (PNP_UDP_1 domain-containing). To study their potential

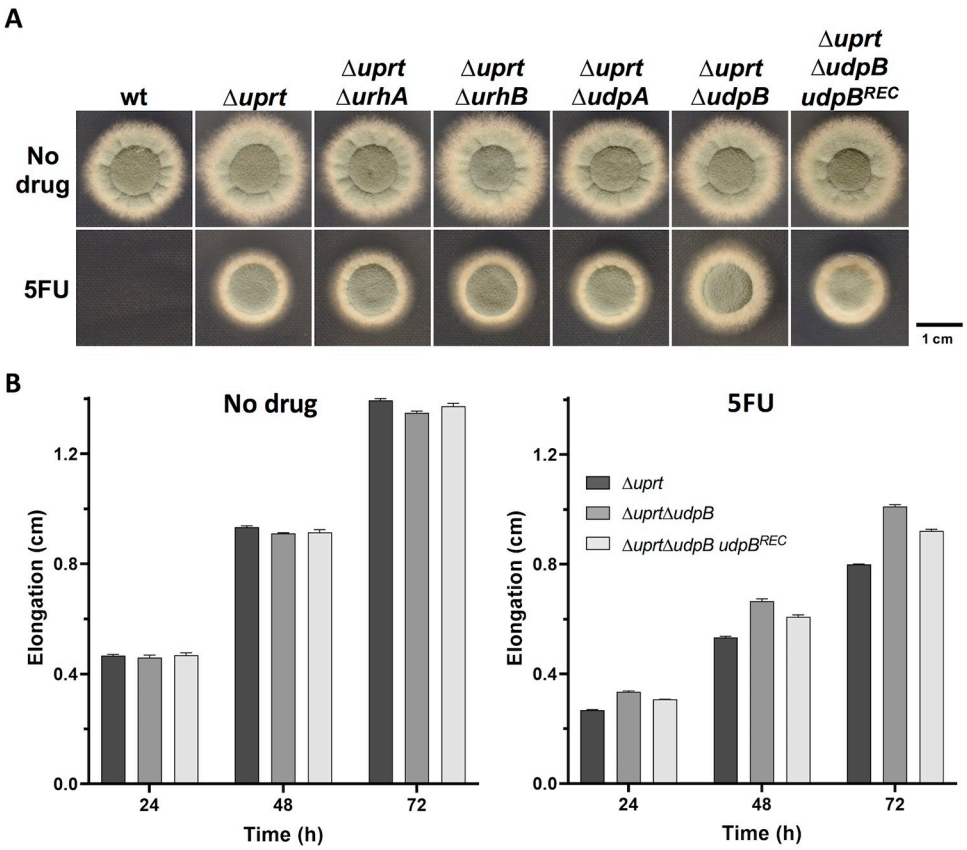

Fig 2. The absence of UdpB increases 5FU resistance in a Uprt deficient background. (A) Radial growth of strains lacking Uprt in combination with enzymes with potential uridine phosphorylase activity was analyzed in the presence of 5FU. **(B)** Colony extension rate analyses confirmed the relevance of UdpB in 5FU toxicity. For both experiments, medium was supplemented with 500 μg/mL of 5FU.

https://doi.org/10.1371/journal.ppat.1011066.g002

role in the conversion of 5FU into 5FUR, the respective genes were, like *urhA* and *urhB*, deleted in Δ*uprt*. While no difference in 5FU resistance could be detected between Δ*uprt* and Δ*uprt*Δ*udpA*, a slight increase in resistance was observed for Δ*uprt*Δ*udpB* (Fig 2A and 2B). Transforming this double mutant with a functional *udpB* gene cassette (Δ*uprt*Δ*udpB udpB*^{REC}), recovered 5FU susceptibility, which further suggests a role of UdpB in the conversion of 5FU into 5FUR. Nevertheless, the small increase in 5FU resistance of Δ*uprt*Δ*udpB* as well as the presence of several further candidate proteins with putative nucleosidase phosphorylase domain indicates that uridine phosphorylase activity is not restricted to a single protein in *A*. *fumigatus*.

During 5FC treatment distinct fluoropyrimidines are generated and extruded

With the exception of UdpB, we found explicit functions of FcyA, Uprt, UrkA and UrhB within the pyrimidine salvage pathway of *A*. *fumigatus* that participate in the metabolization of the fluoropyrimidines 5FC, 5FU and/or 5FUR. Specific, high levels of resistance to these compounds were related to the disruption of individual (Δ*fcyA*, Δ*uprt*, Δ*urkA*) or combinations (Δ*urkA*Δ*urhB*, Δ*uprt*Δ*urkA*) of their encoding genes (Fig 1B).

The absent salvage activities generating the resistance profiles of these mutants are expected to cause an accumulation of 5FC, 5FU and/or 5FUR within the cell. To study this idea and

Table 1. Determination of fluoropyrimidine levels in 5FC treated strains. HPLC-based analysis of **(A)** intra- and **(B)** extracellular 5FC, 5FU and 5FUR levels of 5FC treated wt and pyrimidine salvage pathway mutants with highest degrees of resistance to 5FC, 5FU and/or 5FUR; n.d. not detected.

	A			B		
	5FC	5FU	5FUR	5FC[a]	5FU	5FUR
		nmol/mg ± SD			nmol/mL ± SD	
wt	n.d.	n.d.	0.29 ± 0.02	64.3 ± 4.20	18.0 ± 1.7	n.d.
Δ*fcyA*	1.14 ± 0.06	n.d.	n.d.	85.5 ± 14.8	n.d.	n.d.
Δ*uprt*	n.d.	0.52 ± 0.06	n.d.	35.8 ± 5.00	54.8 ± 9.1	n.d.
Δ*urkA*	n.d.	0.33 ± 0.03	0.18 ± 0.03	57.5 ± 1.50	25.4 ± 2.4	3.4 ± 0.3
Δ*uprt*Δ*urkA*	n.d.	0.50 ± 0.06	n.d.	26.4 ± 3.20	75.6 ± 1.5	n.d.
Δ*urkA*Δ*urhB*	n.d.	n.d.	0.39 ± 0.05	56.2 ± 2.00	19.6 ± 1.6	11.9 ± 0.9

[a]Extracellular 5FC levels constitute a mixture of initially added as well as exported 5FC.

https://doi.org/10.1371/journal.ppat.1011066.t001

investigate whether *A*. *fumigatus* reduces cellular fluoropyrimidine levels by their export into the environment, we measured their intra- and extracellular concentrations in overnight grown liquid cultures that were exposed to 10000 nmol 5FC (100 nmol/mL) for 4 h (**Table 1A** and **1B**).

Δ*fcyA* lacking cytosine deaminase activity showed the highest levels of intra- as well as extracellular 5FC. Neither 5FU nor 5FUR could be detected in this mutant. The highest quantities of intra- as well as extracellular 5FU were observed in mutants lacking Uprt (Δ*uprt*, Δ*uprt*Δ*urkA*), which is in agreement with the role of this enzyme catalyzing the main route of 5FU conversion into 5FUMP. Remarkably, in the culture supernatants of Δ*uprt* and Δ*uprt*Δ*urkA*, 54.8 and 75.6 nmol/mL 5FU were detected, respectively. The largest amount of intra- as well as extracellular levels of 5FUR were detected in Δ*urkA*Δ*urhB* lacking uridine kinase and uridine nucleosidase activities. Despite the block in the direct phosphorylation of 5FUR, Δ*urkA* did not show increased intracellular 5FUR levels compared to wt. However, in contrast to wt an increase in extracellular 5FUR could be detected in Δ*urkA*, which is most likely due to an increased export of 5FUR in mutants lacking this enzyme.

Fluoropyrimidine-efflux during 5FC treatment creates a toxic environment for cytosine deaminase deficient cells

As demonstrated above, during 5FC treatment *A*. *fumigatus* cells reduce intracellular fluoropyrimidine levels through their export into the environment. Like Δ*fcyA*, mammalian cells lack cytosine deaminase and are therefore resistant to 5FC [11]. Both still have the enzymatic capacity to activate 5FU and 5FUR [12, 18], which suggests that the 5FC derived fluoropyrimidine content in supernatants of 5FC treated strains, particularly that of *uprt* deficient strains, could induce toxic effects on both Δ*fcyA* and mammalian cells. To test this idea, different experimental approaches were conducted.

First, wt, Δ*fcyA*, Δ*uprt* and Δ*uprt*Δ*urkA* were grown on solid *Aspergillus* minimal medium (AMM) in the presence of their 5FC treatment derived culture supernatants (**Fig 3A**). Second, a microtiter-based assay was carried out growing strains in liquid AMM to simultaneously quantify and compare their growth in response to each supernatant (**Fig 3B and 3C**). In agreement with Δ*fcyA* not being able to metabolize the supplemented 5FC, its supernatant did not affect its own growth (no inhibition control) and that of Δ*uprt*Δ*urkA*, which is still capable to convert 5FC into 5FU and 5FUR but not 5FUMP. In line with the presence of the alternative route, growth of Δ*uprt* was slightly impaired by the Δ*fcyA* supernatant containing high 5FC levels. Δ*uprt* supernatant, comprising high 5FU, led to a clear growth reduction of Δ*fcyA*. The

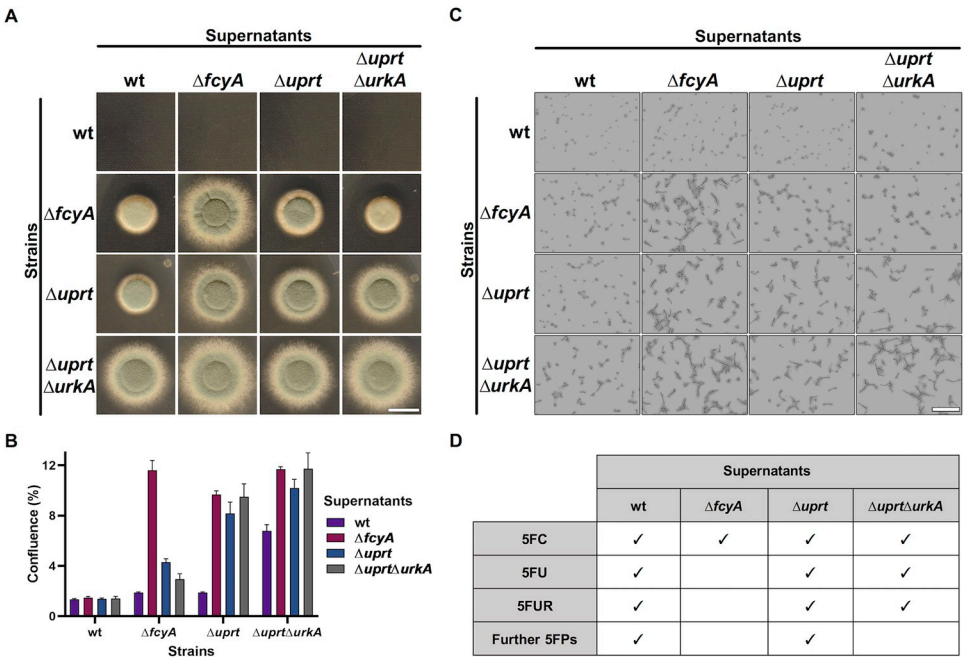

Fig 3. Growth inhibitory effects exerted by effluxed fluoropyrimidines on mutants lacking key pyrimidine salvage activities. (A) Evaluation of the supernatants' impact on the colony growth of strains on solid medium. **(B)** Microtiter-based hyphal growth quantification and **(C)** representative microscopic images illustrating growth of strains in liquid AMM supplemented with distinct supernatants. **(D)** Prediction of the fluoropyrimidine content in supernatants of the respective strains. The susceptibility displayed by Δ*uprt*Δ*urkA* grown in the presence of wt and Δ*uprt* supernatants suggests the efflux of 5FUMP and/or further toxic fluoropyrimidines (5FPs). Scale bars: (A) 1 cm, (C) 100 μm.

https://doi.org/10.1371/journal.ppat.1011066.g003

fluoropyrimidine content of this supernatant slightly blocked growth of Δ*uprt* itself and, surprisingly, that of Δ*uprt*Δ*urkA*. Inhibition of the double mutant, which is anticipated to lack 5FUMP formation out of 5FC, 5FU or 5FUR, suggests that additional 5FC derived inhibitory fluoropyrimidines are generated and exported in Δ*uprt*. *In silico* predictions (https://www.kegg.jp/pathway/afm00240) indicate that *A*. *fumigatus* possesses the enzymatic capacity to generate a large set of fluorinated nucleotides including active metabolites 5-fluorodeoxyuridine monophosphate, 5-fluorodeoxyuridine triphosphate and 5-fluorouridine triphosphate, which could account for these inhibitory effects [33, 34]. Similar to that of Δ*uprt*, supernatant of wt expressing the full set of pyrimidine salvage enzymes, also exhibited activity against Δ*uprt*Δ*urkA*. Furthermore, this supernatant showed high antifungal activity against Δ*fcyA* and Δ*uprt*, which is most likely a result of exported 5FU, 5FUR, 5FUMP and its derived 5-fluorinated nucleotides. Supernatant of Δ*uprt*Δ*urkA*, with the remaining enzymatic capacity to produce 5FU and 5FUR, slightly hampered growth of Δ*uprt* and caused a clear growth inhibition of Δ*fcyA*. In accordance with its lack of enzymes to generate 5FUMP, Δ*uprt*Δ*urkA* was not inhibited by its own supernatant.

In addition to examining the antifungal effects of the different supernatants, we investigated their antiproliferative properties on the human lung carcinoma epithelial cell line A549 [35]. Therefore, A549 cells were incubated in Dulbecco's Modified Eagle Medium (DMEM) supplemented with supernatants of 5FC treated wt, Δ*fcyA*, Δ*uprt* and Δ*uprt*Δ*urkA*. Supernatant of Δ*fcyA* served as control as it should only contain 5FC and thus not induce fluoropyrimidine related inhibitory effects. Two different experimental procedures were tested: in the first, we added the supernatant directly after seeding A549 cells in 96-well plates; while in the second approach the supernatant was added after adherence of the cells. In line with the absence of

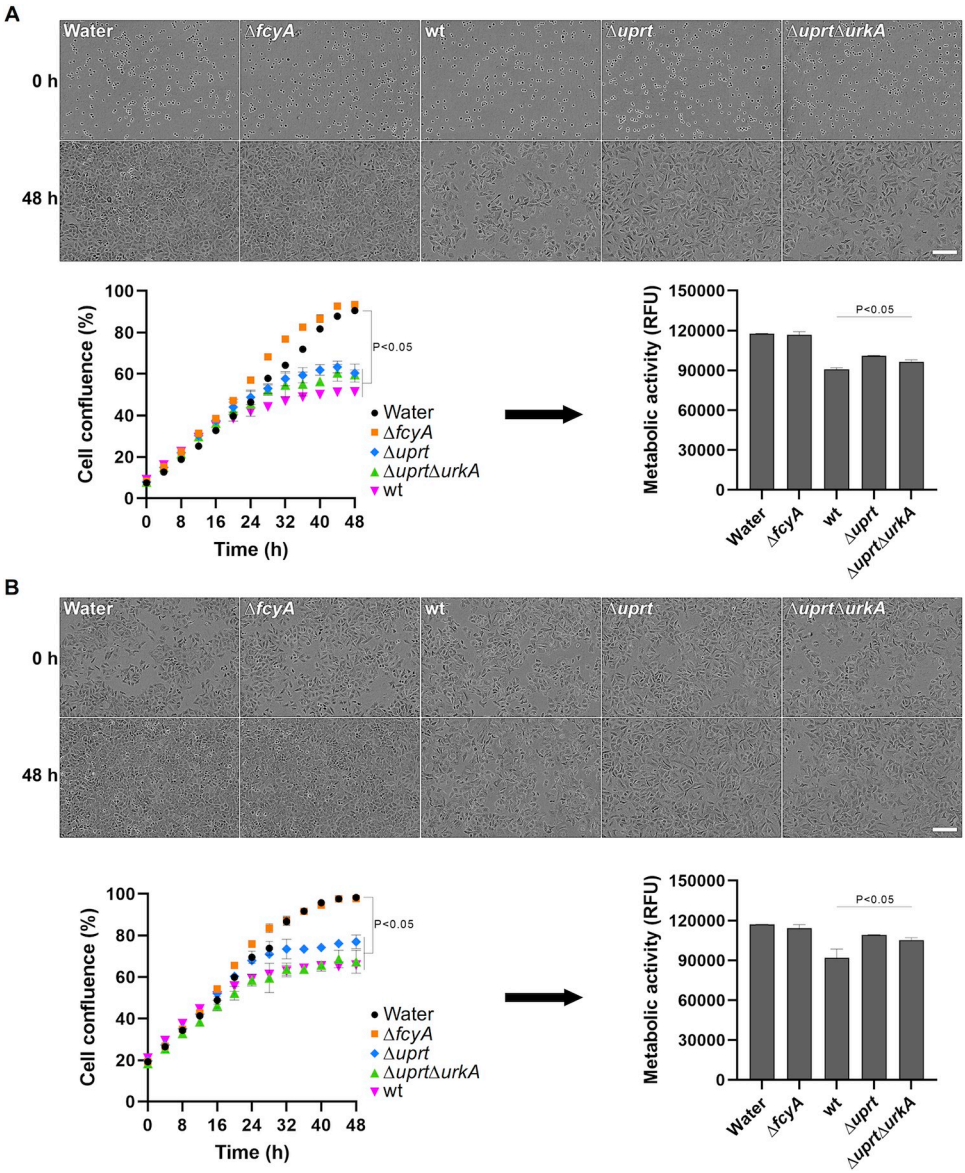

Fig 4. Fungal supernatants containing 5FC-derived antimetabolites compromise proliferation of mammalian cells. Microscopy-assisted analyses and confluence measurements of A549 cells exposed to 5FC treatment derived fungal culture supernatants were performed to determine potential toxic effects. In addition, a resazurin-based assay was carried out after 48 h to measure the metabolic activity of cells. Analyses were performed for cells challenged with the supernatants right after seeding them **(A)** and after cells' adherence **(B)**. Scale bars: 200 μm. RFU, Relative Fluorescence Units.

https://doi.org/10.1371/journal.ppat.1011066.g004

cytosine deaminase, A549 cells showed comparable growth behavior in medium supplemented with Δ*fcyA* supernatant or water (Fig 4A and 4B). Similar to the results obtained for growth of *A. fumigatus* Δ*fcyA*, A549 cells showed the largest growth defects when incubated with supernatants of wt and Δ*uprt*Δ*urkA*, followed by that of Δ*uprt*. We further analyzed viability of A549 cells exposed to supernatants employing a resazurin-based assay [36], which was in agreement with the results obtained by growth analysis. Together, these results led to the suggestion that fluoropyrimidine efflux by *A. fumigatus* could enhance adverse effects on host cells during 5FC antifungal treatment.

Efflux inhibition increases susceptibility to 5-fluoropyrimidines

As stated above, at neutral pH *A*. *fumigatus* displays intrinsic 5FC resistance due to transcriptional downregulation of *fcyB* encoding the major 5FC import protein in this fungus [15]. Based on our data we suspected efflux-mediated intracellular reduction of fluoropyrimidines during 5FC treatment to be an additional factor contributing to 5FC tolerance that could be overcome by its inhibition. To test this idea, we investigated synergistic interactions of 5FC, 5FU and 5FUR with the fungal ABC and MFS efflux pump inhibitor CLG [19, 20]. For this, checkerboard assays coupled with high-throughput microscopic analysis were employed. Based on the growth inhibitory action of each compound as well as their combinations, Bliss synergy scores were calculated using the SynergyFinder Plus tool [37, 38]. For each 5FC, 5FU and 5FUR, synergistic interaction with CLG was found at various combinations (**Fig 5A and 5B**, and **Tables A and B in S3 Table**). The 10 highest scores were determined using CLG at a concentration of 12.5 and 25 μg/mL after 24 h as well as 25 and 50 μg/mL after 48 h. On their own for instance, visually assessed MIC levels of 5FC and 5FU were 200 and 50 μg/mL after 24 h as well as 400 and 100 μg/mL after 48 h. Despite the obvious antifungal activity of 5FUR, even at a concentration level of 2000 μg/mL wt was still able to grow and therefore, no MIC could be determined for this drug. In combination with 25 μg/mL CLG, we detected MICs for 5FC, 5FU and 5FUR of 25, 6.25 and 62.5 μg/mL after 24 h, and 25, 6.25 and 250 μg/mL after 48

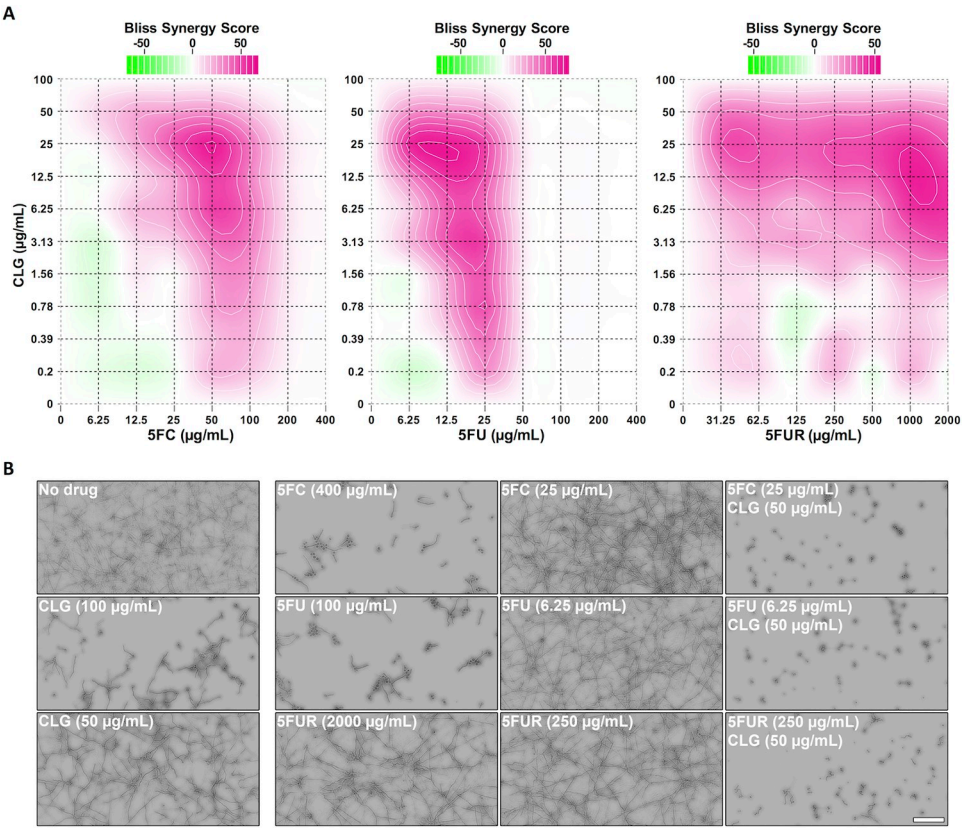

Fig 5. CLG potentiates 5FC, 5FU and 5FUR antifungal activity against *A*. *fumigatus*. **(A)** Checkerboard assays using 5FC, 5FU or 5FUR in combination with CLG were carried out to determine Bliss synergy scores (24 h). **(B)** Microscopic images of wells (48 h) corresponding to the visually detected MICs of each fluoropyrimidine and CLG in single use as well as their combination requiring the lowest 5FC, 5FU or 5FUR amounts to prevent fungal growth. Checkerboard assays were performed in RPMI medium. Scale bar: 100 μm.

https://doi.org/10.1371/journal.ppat.1011066.g005

h using 50 μg/mL CLG. The large increase of 5FC activity (up to 16-fold) in the presence of CLG indicates fluoropyrimidine export as a mechanism in *A*. *fumigatus* that significantly lowers 5FC activity, which can be overcome by combinatorial treatment.

Discussion

5FC metabolic activation starts with the formation of the nucleotide 5FUMP and, in *A*. *fumigatus*, this process is predominantly mediated by cytosine deaminase (FcyA) and uracil phosphoribosyltransferase (Uprt) [12]. In this work, we identified three further enzymes with pyrimidine salvage activities including uridine phosphorylase (UdpB), uridine nucleosidase (UrhB) and uridine kinase (UrkA), which mediate the metabolization of 5FC derivatives 5FU and/or 5FUR. Two of them, uridine phosphorylase and uridine kinase, enable an alternative enzymatic route of 5FC metabolic activation in which 5FU, the reaction product of cytosine deaminase, is converted to 5FUMP *via* 5FUR (Fig 6). Interestingly, in contrast to *udpB* which appears functionally redundant for the conversion of 5FU into 5FUR, *fcyA*, *uprt*, *urkA* and *urhB* encode the major proteins catalyzing their corresponding enzymatic steps and, according to previous work, they are part of the *A*. *fumigatus* core genome [39, 40].

During 5FC treatment, the metabolic blocks caused by the absence of specific pyrimidine salvage activities resulted in increased intracellular accumulation of either 5FC (Δ*fcyA*), 5FU (Δ*uprt* and Δ*uprt*Δ*urkA*) or 5FUR (Δ*urkA*Δ*urhB*), which was accompanied by their elevated efflux into the environment. Particularly mutants lacking Uprt, catalyzing the major and direct route of 5FUMP formation, showed excessive extracellular 5FU levels in their culture supernatants after 5FC exposure. To further conclude about the effluxed fluoropyrimidine composition of Uprt mutants as well as that of Δ*fcyA* (5FC accumulation control) and wt expressing the full set of pyrimidine salvage enzymes, growth inhibition assays were performed using medium supplemented with their supernatants (Fig 3). In this regard it has to be mentioned

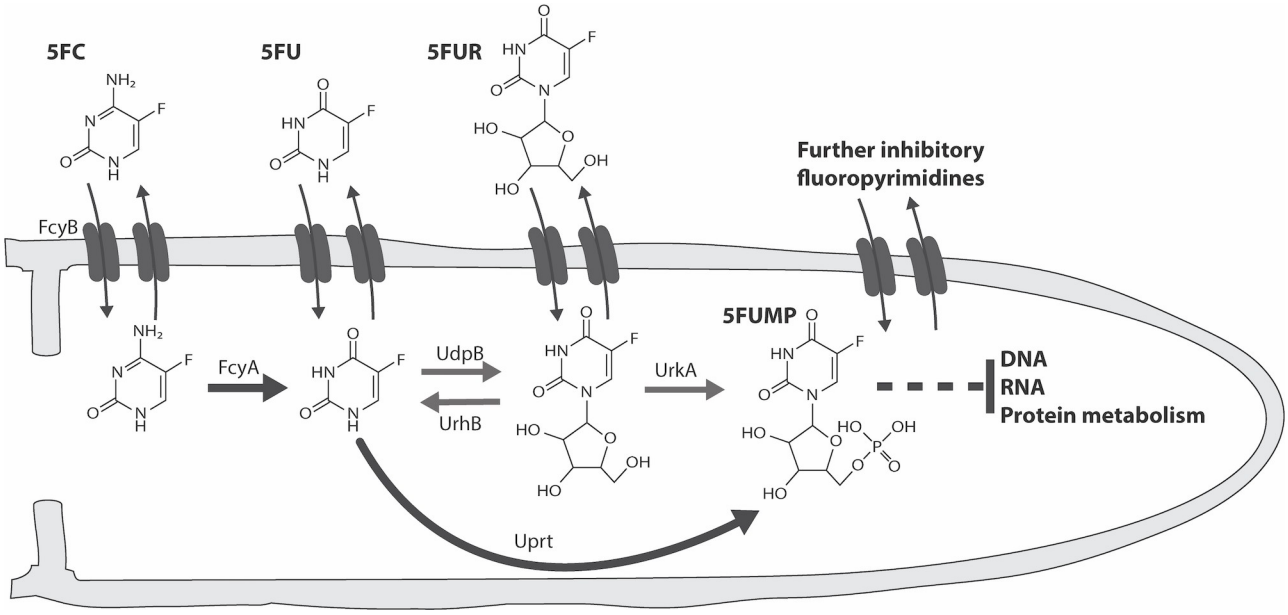

Fig 6. Proposed model illustrating transport dynamics and pyrimidine salvage activities that mediate the metabolic conversion of fluoropyrimidines in *A*. *fumigatus*. The major route of 5FC metabolic activation is catalyzed by FcyA and Uprt (black arrows). UdpB, UrhB and UrkA constitute enzymes of a metabolic bypass (grey arrows) that generates 5FUMP, however in a less efficient way. During 5FC treatment, intracellular levels of 5FC, 5FU, 5FUR and so far unknown fluoropyrimidine antimetabolites are reduced by their export into the environment.

https://doi.org/10.1371/journal.ppat.1011066.g006

that in contrast to Δ*uprt*Δ*urkA*, both wt and Δ*uprt* possess the enzymatic capacity to generate 5FUMP, which represents the precursor of various active 5-fluorinated nucleotides. Susceptibility profiles of wt, Δ*fcyA*, Δ*uprt* and Δ*uprt*Δ*urkA* suggested the efflux of 5FU and 5FUR by Δ*uprt*Δ*urkA*, together with so far unidentified toxic fluoropyrimidines by wt and Δ*uprt*.

As stated above, 5FC is considered non-toxic for mammalian cells due to the absence of cytosine deaminase [11]. Yet, toxic effects are occurring during 5FC treatment that were, at least in part, associated with the capacity of members of the human microbiome to convert 5FC into the chemotherapeutic agent 5FU [41, 42]. The composition of microbial species and their expressed salvage activities as well as their location within the body probably constitute several factors that could influence 5FC related host toxicity. *E. coli*, a common member of human microbiome [42], for instance expresses cytosine deaminase [43], uracil phosphoribosyltransferase [44], uridine phosphorylase [27] as well as uridine kinase [45], which should enable the conversion of 5FC into 5FU, 5FUR, 5FUMP as well as further derivatives thereof. Thus, it is very likely that in addition to 5FU, a variety of other 5FC derived cytotoxic compounds will be generated and released by the human microbiome during 5FC exposure. We hypothesized that, in addition to the fluoropyrimidines produced by the microbiome, those produced by pathogens could enhance adverse effects on host cells during infections involving 5FC treatment. Using culture supernatants of 5FC exposed wt and Uprt deficient mutants, in this work we demonstrate the capacity of *A. fumigatus* to generate and release fluoropyrimidines that compromise proliferation of A549 cells (**Fig 4**). We speculate that similar fluoropyrimidine detoxifying mechanisms than those observed for *A. fumigatus* could be present in clinical yeast, which remains to be investigated. Importantly, mutations affecting uracil phosphoribosyltransferase activity are a major reason for cross-resistance to 5FC and 5FU in *Candida* and *Cryptococcus* species [11].

In previous work we elucidated transcriptional repression of 5FC uptake and the consequent reduced 5FC import as the major mechanism conferring high 5FC tolerance in *A. fumigatus* at neutral pH [15]. Here, we uncover fluoropyrimidine efflux as an additional factor that diminishes 5FC activity in this mold pathogen. Based on the hypothesis that 5FC activity could be enhanced by perturbing fluoropyrimidine export, we employed 5FC as well as its effluxed derivatives 5FU and 5FUR in combination with the fungal efflux pump inhibitor CLG and identified strong synergistic interactions between CLG and all three compounds. The fluoropyrimidine export-driven decrease in 5FC antifungal activity as well as the toxic effects on host cell proliferation, suggests targeting fungal efflux during 5FC treatment as a promising therapeutic strategy. Findings of this study should prompt future research towards efflux-based mechanisms and strategies to prevent them, including the assessment of the proposed mechanisms *in vivo*, particularly in fungal species where this nucleobase analog is still a favorable treatment option.

Material and methods

Growth conditions for phenotypic analyses and fungal transformation

Generally, AMM [46] containing 100 mM MOPS buffer (pH 7), 20 mM ammonium tartrate as nitrogen source and 1% glucose as carbon source was used for phenotypic analyses. Plate growth assays were conducted on solid AMM containing 1.5% agar (Carl Roth GmbH, Karlsruhe, Germany). Cultures were generally grown at 37˚C. Three independent experiments were carried out for phenotypical analyses.

Plate growth-based susceptibility testing of mutants was assessed in solid AMM. 10^4 spores in a total volume of 5 μL spore buffer (0.1% Tween 20, 0.9% sodium chloride solution (*w/v*)) were point inoculated on solid AMM supplemented with 5FC, 5FU or 5FUR (Tokyo Chemical

Industry, Tokyo, Japan) and incubated for 48 h. Colony extension measurements were performed by inoculating the respective strain on the edge of AMM plates. Subsequently, the mean of the colony extension rate was calculated after measuring five vertical transects on the edge of the colony coverage area every 24 h for a final period of three days. Microtiter-based liquid cultures were performed in Nunc96 microplates (Thermo Scientific Inc., Waltham, MA, USA). Each well contained 10^4 spores in a total volume of 100 μL medium.

For fungal transformation, solid AMM with 1 M sucrose and 0.7% agar was used. Solid Sabouraud dextrose (SAB, Sigma-Aldrich Corp., St. Louis, MI, USA) medium with 1.5% agar was used for the generation of spores. Fungal genetic manipulations were carried out using 1 μg of the corresponding DNA construct which was transformed into the respective recipients. Selection procedures using conventional selectable marker genes were conducted as described previously for *A*. *fumigatus* [47].

Deletion of *A. fumigatus urkA*, *urhA*, *urhB*, *udpA* and *udpB*

The strains and primers used in this study are listed in **S4** and **S5** **Tables**, respectively. Generally, the CEA10 Δ*ku80* derivative A1160P+, here termed wt, was used as parental strain. To generate knock-out mutants, the coding sequence of the corresponding gene was disrupted using hygromycin B, phleomycin and pyrithiamine resistance cassettes. Therefore, deletion constructs comprising approximately 1 kb of the respective 5′ and 3′ nontranslated regions (NTRs) linked to the central antibiotic resistance cassette were generated using fusion PCR as previously described [48]. Correct integration of transformed constructs was confirmed by Southern blot analysis.

Reconstitution of the Δ*urkA*, Δ*urhB* and Δ*udpB* mutants

To complement the Δ*urkA*, Δ*urhB* and Δ*udpB* mutant phenotypes, plasmids pFG66, pFG67 and pESV38 were generated (**S6 Table**). The strategy used to complement mutants lacking different pyrimidine salvage activities is illustrated in **S2 Fig**. First, the coding sequences plus approximately 1-kb 5′ and 3′ of their respective NTRs were amplified using primers urkA-compl-FW/-RV, urhBcompl-FW/RV and udpBcompl-FW/RV. Second, the backbone of the pyrithiamine resistance-conferring plasmid pSK275 [49] was amplified with the primer pair BBpSK275-FW/RV. After PCR-purification, all PCR products were assembled into the pSK275 backbone using the NEBuilder HiFi DNA assembly Master Mix (New England Biolabs, Ipswich, MA, USA), and the constructs were propagated in *E*. *coli*. Around 1 μg of the pFG66, pFG67 and pESV38 plasmids were linearized by restriction digestion with *Eco*RV, *Hpa*I and *Mlu*I respectively and used as templates to transform into the corresponding genetic background.

Efflux-based growth inhibition assays

Supernatants from wt, Δ*fcyA*, Δ*uprt* and Δ*uprt*Δ*urkA* grown in the presence of 5FC were recovered. For this, 100 mL of liquid AMM were inoculated with 1×10^6/mL spores of each strain and incubated at 37˚C for 16 h shaking at 200 rpm. Cultures were then supplemented with 250 μg/mL of 5FC and incubated for further 10 h before collecting. Before sterile filtration, the supernatants were incubated at 80˚C for 1 h to prevent metabolic activities. For susceptibility testing on solid and in liquid medium, 1 volume of 2×AMM buffered with 100 mM of MOPS (pH 7) was combined with 1 volume of each supernatant. Microtiter-based growth in liquid medium was monitored during early-stage growth (8 h) with the IncuCyte S3 Live-Cell Analysis System (Essen Bioscience Inc., Ann Arbor, MI, USA) using the 20× magnification S3/SX1 G/R Optical Module. From each well, two images were taken from the central

area of the well. Fungal growth was analyzed using the Basic Analyzer software of the IncuCyte S3 (Confluence %, Segmentation adjustment: 0.1, Adjust size: -1).

Cell culture and proliferation assay

The human lung carcinoma epithelial cell line A549 (American type culture collection, CCL-185) was maintained by serial passage in DMEM/F-12 (Sigma-Aldrich Corp., St. Louis, MI, USA) with 10% FBS (Sigma-Aldrich Corp., St. Louis, MI, USA). For the proliferation assay, cells were seeded at a concentration of 1×10^5 cells/mL in Corning 96-well black polystyrene microplates with clear bottom (Fischer Scientific, Illkirch, France) and cultured at 37˚C and 5% CO_2. Cells were challenged with 5 μL supernatant (1:20 dilution) collected from 5FC exposed wt, Δ*fcyA*, Δ*uprt* and Δ*uprt*Δ*urkA* liquid cultures. Supernatant was added either immediately after seeding or after cells adhered, which consistently occurred after 6 h. Proliferation of A549 cells was monitored over the duration of 48 h with the IncuCyte S3 Live-Cell Analysis System. Four images per well were acquired every 2 h. For A549 cells, the magnification required with the S3/SX1 G/R Optical Module was 10×. Cell confluence was determined using the Basic Analyzer software of the IncuCyte S3 for phase imaging.

Resazurin-based assay was performed as previously described [36] with few modifications. For this, cells were incubated in the presence of supernatants for 48 h before adding 50 μM resazurin for another 4 h. Subsequently, fluorescence measurements were performed using the CLARIOstar Plus microplate reader (BMG LABTECH, Ortenberg, Germany) with excitation at 544 nm and emission at 590 nm. All experiments have been performed in triplicates.

Checkerboard assays and synergy analyses

To study the relevance of efflux pumps on fluoropyrimidine resistance, drug interaction assays were performed by the microdilution checkerboard method [50]. Checkerboards were performed in RPMI medium (pH 7), (Sigma-Aldrich Corp., St. Louis, MI, USA), combining 5FC, 5FU or 5FUR with CLG (Sigma-Aldrich Corp., St. Louis MI, USA) against *A*. *fumigatus* wt. The final concentration of 5FC and 5FU ranged from 6.25 to 400 μg/mL, whereas 5FUR and CLG concentrations ranged from 31.25 to 2000 μg/mL and 0.20 to 100 μg/mL, respectively. In brief, 10 μL of each compound dilution was mixed with 80 μL of 1.25×RPMI medium containing 1.25×10^5 spores/mL, to obtain a final volume of 100 μL of 1×medium with 1×10^5 spores/mL. Microscopy-based growth quantification was carried out using the Basic Analyzer software from the IncuCyte S3 Live-Cell Analysis System as described above for the efflux-based growth inhibition assay. To overcome autofocus imprecisions and further inaccuracies in growth measurements, due to extensive vertical growth after long-term incubation [51], confluence was determined after both 24 and 48 h of treatment. The Bliss Independence Model [37] was used to analyze the potential synergistic interactions among the different drug combinations for both time points. In this model antagonistic interactions are estimated to produce scores less than 10, whereas scores from -10 to 10 are consequence of additive interactions. Scores larger than 10 suggest synergistic interactions. In addition to Bliss scores, the Fractional Inhibitory Concentration Index [52] was determined to further evaluate synergistic interactions.

Fluoropyrimidine quantification

Intra- and extracellular fluoropyrimidine levels of pyrimidine salvage mutants were quantified by High Performance Liquid Chromatography coupled with Variable Wavelength Detector (HPLC-VWD). For this, 1×10^6 spores/mL of each strain were inoculated in 100 mL of AMM for 16 h. Cultures were then supplemented with 100 nmol/mL of 5FC for further 4 h.

Mycelium and supernatant 5FC treated cultures were collected by filtration. Both supernatant and mycelia samples were incubated in a water bath at 80˚C for 1 h before analysis.

Then, 10 mg of dried mycelium were powderized, mixed with 400 μL water and vortexed with two glass beads for 15 min. The mixture was centrifuged for 10 min at 10,000 g and the supernatant was analyzed by HPLC-VWD using an Agilent Series 1100 HPLC system (Agilent Technologies Deutschland GmbH, Waldbronn, Germany). Chromatographic separation was carried out with an Agilent Zorbax Eclipse Plus C18 (150×4.6 mm, i.d. 5.0 μm) column (Agilent Technologies Deutschland GmbH, Waldbronn, Germany). The mobile phase was a mixture of water with 0.0001% 1-octanesulfonic acid sodium salt (*w/v*) [53] (A) and methanol (B). The gradient started with 1% (B), followed by 2.5% at 4 min, and by 15% at 4 min. The total run time including column equilibration was 15 min with a flow rate at 1.2 mL/min, and an injection volume of 10 μL. The column oven was set at 22˚C. The UV detection wavelength was set at 280 nm. Data analysis and instrument control was carried out with Thermo Scientific Dionex Chromeleon 7.2 Chromatography Data System (Thermo Fisher Scientific, Dreieich, Germany). The retention times were 2.4 min for 5FC, 2.9 min for 5FU, and 7.2 min for 5FUR. The concentration of each compound was determined using external standard calibration.

Statistical analysis

GraphPad Prism 9 software (Dotmatics, Boston, MA, USA) was used to analyze and display statistic results. All experiments were performed using three biological replicates. Experiments considering two independent variables (*Aspergillus fumigatus* supernatant and A549 cell line) were analyzed using a two-way ANOVA with Dunnett multiple comparison test. All graphs depict the mean, and the error bars show the standard deviation. *P*-values of $\leq$0.05 were considered as significant.

The numerical data used in tables and figures are included in S1 Data.

Supporting information

S1 Fig. Plate growth-based susceptibility testing of *urkA*, *urhA* and *urhB* mutants with predicted defects in 5FUR/uridine metabolization. 5FUR resistance of deletion mutants as well as complemented versions (*REC*) was assessed on solid medium supplemented with 500 μg/mL of 5FUR.
(TIF)

S2 Fig. Schematic illustration of the strategy used to generate pyrimidine-salvage knock out and complemented mutants. Plasmid for the reconstitution were linearized for site-directed insertion at the corresponding deletion locus.
(TIF)

S1 Table. Protein-based BLAST analyses (https://blast.ncbi.nlm.nih.gov/Blast.cgi) of *S. cerevisiae* (S288C) uridine kinase Urk1p (YNR012W) and uridine nucleosidase Urh1p (YDR400W) against *A. fumigatus* (A1163). (A) BLASTP analysis suggested one Urk1p ortholog in *A. fumigatus*. **(B)** Two orthologs of *S. cerevisiae* Urh1p were predicted, which we termed UrhA and UrhB. Despite the higher homology, resistance analysis (**Figs 1** and **S1**) confirmed uridine nucleosidase activity for UrhB but not UrhA.
(DOCX)

S2 Table. Domain analyses performed with the InterPro database (https://www.ebi.ac.uk/interpro/) revealed 10 proteins carrying a predicted nucleoside phosphorylase domain (IPR000845) in *A. fumigatus* A1163. Proteins with a putative purine nucleoside

phosphorylase and uridine phosphorylase domains (PNP_UDP_1; PF01048) are highlighted in bold.
(DOCX)

S3 Table. CLG exerts synergistic interaction with each 5FC, 5FU and 5FUR. Bliss scores were generated to assess potential synergism between CLG and fluoropyrimidines. For drug combinations yielding the 10 highest scores, MICs were visually determined and used for the calculation of the Fractional Inhibitory Concentration Index (FICI). Checkerboard assays were performed in RPMI and evaluated after 24 h **(A)** and 48 h **(B)**.
(DOCX)

S4 Table. Strains used in this study.
(DOCX)

S5 Table. Oligonucleotides used in this study.
(DOCX)

S6 Table. Plasmids used in this study.
(DOCX)

S1 Data. Underlying raw data for Tables 1A, 1B, A and B in S3 Table as well as Figs 2B, 3B, 4A, 4B and 5A.
(XLSX)

Acknowledgments

The authors would like to thank Johanna Gostner for supplying A549 cells and F2G for providing olorofim. Anna Niedrig and Christoph Müller thank Prof. Dr. Franz Bracher for providing his laboratories and equipment. L.E. S.-V. participated in the HOROS program W1253 funded by the FWF.

Author Contributions

Conceptualization: Fabio Gsaller.

Data curation: Luis Enrique Sastré-Velásquez, Alex Dallemulle, Alexander Kühbacher, Clara Baldin, Anna Niedrig, Christoph Müller, Fabio Gsaller.

Formal analysis: Luis Enrique Sastré-Velásquez, Alex Dallemulle, Alexander Kühbacher, Clara Baldin, Anna Niedrig, Christoph Müller, Fabio Gsaller.

Funding acquisition: Clara Baldin, Fabio Gsaller.

Investigation: Luis Enrique Sastré-Velásquez, Alex Dallemulle, Alexander Kühbacher, Clara Baldin, Laura Alcazar-Fuoli, Christoph Müller, Fabio Gsaller.

Methodology: Luis Enrique Sastré-Velásquez, Alexander Kühbacher, Clara Baldin, Laura Alcazar-Fuoli, Anna Niedrig, Christoph Müller, Fabio Gsaller.

Project administration: Fabio Gsaller.

Resources: Fabio Gsaller.

Supervision: Fabio Gsaller.

Visualization: Luis Enrique Sastré-Velásquez, Fabio Gsaller.

Writing – original draft: Luis Enrique Sastré-Velásquez, Fabio Gsaller.

Writing – review & editing: Luis Enrique Sastré-Velásquez, Alexander Kühbacher, Clara Baldin, Laura Alcazar-Fuoli, Christoph Müller, Fabio Gsaller.

References

1. Brown GD, Denning DW, Gow NAR, Levitz SM, Netea MG, White TC. Hidden killers: human fungal infections. Sci Transl Med. 2012; 4(165):165rv13. https://doi.org/10.1126/scitranslmed.3004404 PMID: 23253612.
2. Bongomin F, Gago S, Oladele RO, Denning DW. Global and multi-national prevalence of fungal diseases-estimate precision. J Fungi (Basel). 2017; 3(4). https://doi.org/10.3390/jof3040057 PMID: 29371573.
3. Krishnan S, Manavathu EK, Chandrasekar PH. *Aspergillus flavus*: an emerging non-fumigatus *Aspergillus* species of significance. Mycoses. 2009; 52(3):206–22. https://doi.org/10.1111/j.1439-0507.2008.01642.x PMID: 19207851.
4. Latgé JP. *Aspergillus fumigatus* and aspergillosis. Clin Microbiol Rev. 1999; 12(2):310–50. https://doi.org/10.1128/cmr.12.2.310 PMID: 10194462.
5. Latgé JP, Chamilos G. *Aspergillus fumigatus* and aspergillosis in 2019. Clin Microbiol Rev. 2019; 33(1). https://doi.org/10.1128/CMR.00140-18 PMID: 31722890.
6. Perfect JR, Cox GM, Lee JY, Kauffman CA, de Repentigny L, Chapman SW, et al. The impact of culture isolation of *Aspergillus* species: a hospital-based survey of aspergillosis. Clin Infect Dis. 2001; 33 (11):1824–33. https://doi.org/10.1086/323900 PMID: 11692293.
7. Ullmann AJ, Aguado JM, Arikan-Akdagli S, Denning DW, Groll AH, Lagrou K, et al. Diagnosis and management of *Aspergillus* diseases: executive summary of the 2017 ESCMID-ECMM-ERS guideline. Clin Microbiol Infect. 2018; 24:e1–e38. https://doi.org/10.1016/j.cmi.2018.01.002 PMID: 29544767.
8. Patterson TF, Thompson GR 3rd, Denning DW, Fishman JA, Hadley S, Herbrecht R, et al. Executive summary: practice guidelines for the diagnosis and management of aspergillosis: 2016 update by the infectious diseases society of America. Clin Infect Dis. 2016; 63(4):433–42. https://doi.org/10.1093/cid/ciw444 PMID: 27481947.
9. Verweij PE, te Dorsthorst DTA, Janssen WHP, Meis JFGM, Mouton JW. *In vitro* activities at pH 5.0 and pH 7.0 and *in vivo* efficacy of flucytosine against *Aspergillus fumigatus*. Antimicrob Agents Chemother. 2008; 52(12):4483–5. https://doi.org/10.1128/AAC.00491-08 PMID: 18794382.
10. te Dorsthorst DTA, Verweij PE, Meis JF, Mouton JW. Efficacy and pharmacodynamics of flucytosine monotherapy in a nonneutropenic murine model of invasive aspergillosis. Antimicrob Agents Chemother. 2005; 49(10):4220–6. https://doi.org/10.1128/AAC.49.10.4220-4226.2005 PMID: 16189101.
11. Delma FZ, Al-Hatmi AMS, Brüggemann RJM, Melchers WJG, de Hoog S, Verweij PE, et al. Molecular mechanisms of 5-fluorocytosine resistance in yeasts and filamentous fungi. J Fungi (Basel). 2021; 7 (11). https://doi.org/10.3390/jof7110909 PMID: 34829198.
12. Birštonas L, Dallemulle A, Lopez-Berges MS, Jacobsen ID, Offterdinger M, Abt B, et al. Multiplex genetic engineering exploiting pyrimidine salvage pathway-based endogenous counterselectable markers. mBio. 2020; 11(2). https://doi.org/10.1128/mBio.00230-20 PMID: 32265325.
13. Billmyre RB, Applen Clancey S, Li LX, Doering TL, Heitman J. 5-fluorocytosine resistance is associated with hypermutation and alterations in capsule biosynthesis in *Cryptococcus*. Nat Commun. 2020; 11 (1):127. https://doi.org/10.1038/s41467-019-13890-z PMID: 31913284.
14. Costa C, Ponte A, Pais P, Santos R, Cavalheiro M, Yaguchi T, et al. New mechanisms of flucytosine resistance in *C. glabrata* unveiled by a chemogenomics analysis in *S. cerevisiae*. PLoS One. 2015; 10 (8):e0135110. https://doi.org/10.1371/journal.pone.0135110 PMID: 26267134.
15. Gsaller F, Furukawa T, Carr PD, Rash B, Jochl C, Bertuzzi M, et al. Mechanistic basis of pH-dependent 5-flucytosine resistance in *Aspergillus fumigatus*. Antimicrob Agents Chemother. 2018; 62(6). https://doi.org/10.1128/AAC.02593-17 PMID: 29610197.
16. Alexander BD, Procop GW, Dufresne P, Espinel-Ingroff A, Fuller J, Ghannoum MA, et al. Reference method for broth dilution antifungal susceptibility testing of filamentous fungi. CLSI standard M38. 3rd edition: Clinical and Laboratory Standards Institute (CLSI); 2017.
17. Guinea J, Meletiadis J, Arikan-Akdagli S, Muehlethaler K, Kahlmeter G, Arendrup MC, et al. Method for the determination of broth dilution minimum inhibitory concentrations of antifungal agents for conidia forming moulds 2022. Available from: https://www.eucast.org/fileadmin/src/media/PDFs/EUCAST_files/AFST/Files/EUCAST_EDef_9.4_method_for_susceptibility_testing_of_moulds.pdf.
18. Longley DB, Harkin DP, Johnston PG. 5-Fluorouracil: mechanisms of action and clinical strategies. Nat Rev Cancer. 2003; 3(5):330–8. https://doi.org/10.1038/nrc1074 PMID: 12724731.

19. Holmes AR, Keniya MV, Ivnitski-Steele I, Monk BC, Lamping E, Sklar LA, et al. The monoamine oxidase A inhibitor clorgyline is a broad-spectrum inhibitor of fungal ABC and MFS transporter efflux pump activities which reverses the azole resistance of *Candida albicans* and *Candida glabrata* clinical isolates. Antimicrob Agents Chemother. 2012; 56(3):1508–15. https://doi.org/10.1128/AAC.05706-11 PMID: 22203607.

20. Esquivel BD, Rybak JM, Barker KS, Fortwendel JR, Rogers PD, White TC. Characterization of the efflux capability and substrate specificity of *Aspergillus fumigatus* PDR5-like ABC transporters expressed in *Saccharomyces cerevisiae*. mBio. 2020; 11(2). https://doi.org/10.1128/mBio.00338-20 PMID: 32209680.

21. Mitterbauer R, Karl T, Adam G. *Saccharomyces cerevisiae* URH1 (encoding uridine-cytidine N-ribohydrolase): functional complementation by a nucleoside hydrolase from a protozoan parasite and by a mammalian uridine phosphorylase. Appl Environ Microbiol. 2002; 68(3):1336–43. https://doi.org/10.1128/AEM.68.3.1336-1343.2002 PMID: 11872485.

22. Oliver JD, Sibley GEM, Beckmann N, Dobb KS, Slater MJ, McEntee L, et al. F901318 represents a novel class of antifungal drug that inhibits dihydroorotate dehydrogenase. Proc Natl Acad Sci U S A. 2016; 113(45):12809. https://doi.org/10.1073/pnas.1608304113 PMID: 27791100.

23. Kurtz JE, Exinger F, Erbs P, Jund R. The *URH1* uridine ribohydrolase of *Saccharomyces cerevisiae*. Curr Genet. 2002; 41(3):132–41. https://doi.org/10.1007/s00294-002-0296-9 PMID: 12111094.

24. Pritchard RH, Ahmad SI. Fluorouracil and the isolation of mutants lacking uridine phosphorylase in *Escherichia coli*: location of the gene. Mol Gen Genet. 1971; 111(1):84–8. https://doi.org/10.1007/BF00286557 PMID: 4932245.

25. Lashkov AA, Zhukhlistova NE, Seregina TA, Gabdulkhakov AG, Mikhailov AM. Uridine phosphorylase in biomedical, structural, and functional aspects: a review. Crystallogr Rep. 2011; 56(4):560. https://doi.org/10.1134/S1063774511040122

26. Yang C, Li J, Huang Z, Zhang X, Gao X, Zhu C, et al. Structural and catalytic analysis of two diverse uridine phosphorylases in Phytophthora capsici. Sci Rep. 2020; 10(1):9051. https://doi.org/10.1038/s41598-020-65935-9 PMID: 32493959.

27. Leer JC, Hammer-Jespersen K, Schwartz M. Uridine Phosphorylase from *Escherichia coli*. Physical and chemical characterization. Eur J Biochem. 1977; 75(1):217–24. 16751.

28. Watanabe S, Uchida T. Cloning and expression of human uridine phosphorylase. Biochem Biophys Res Commun. 1995; 216(1):265–72. https://doi.org/10.1006/bbrc.1995.2619 PMID: 7488099.

29. Johansson M. Identification of a novel human uridine phosphorylase. Biochem Biophys Res Commun. 2003; 307(1):41–6. https://doi.org/10.1016/s0006-291x(03)01062-3 PMID: 12849978.

30. Apweiler R, Attwood TK, Bairoch A, Bateman A, Birney E, Biswas M, et al. The InterPro database, an integrated documentation resource for protein families, domains and functional sites. Nucleic Acids Res. 2001; 29(1):37–40. https://doi.org/10.1093/nar/29.1.37 PMID: 11125043.

31. Blum M, Chang H-Y, Chuguransky S, Grego T, Kandasaamy S, Mitchell A, et al. The InterPro protein families and domains database: 20 years on. Nucleic Acids Res. 2021; 49(D1):D344–D54. https://doi.org/10.1093/nar/gkaa977 PMID: 33156333.

32. Bertuzzi M, van Rhijn N, Krappmann S, Bowyer P, Bromley MJ, Bignell EM. On the lineage of *Aspergillus fumigatus* isolates in common laboratory use. Med Mycol. 2020; 59(1):7–13. https://doi.org/10.1093/mmy/myaa075 PMID: 32944768.

33. Kanehisa M. Toward understanding the origin and evolution of cellular organisms. Protein Sci. 2019; 28(11):1947–51. https://doi.org/10.1002/pro.3715 PMID: 31441146.

34. Kanehisa M, Furumichi M, Sato Y, Kawashima M, Ishiguro-Watanabe M. KEGG for taxonomy-based analysis of pathways and genomes. Nucleic Acids Res. 2022. Epub 2022/10/28. https://doi.org/10.1093/nar/gkac963 PMID: 36300620.

35. Giard DJ, Aaronson SA, Todaro GJ, Arnstein P, Kersey JH, Dosik H, et al. *In vitro* cultivation of human tumors: establishment of cell lines derived from a series of solid tumors. J Natl Cancer Inst. 1973; 51(5):1417–23. https://doi.org/10.1093/jnci/51.5.1417 PMID: 4357758.

36. Balbaied T, Moore E. Resazurin-Based Assay for Quantifying Living Cells during Alkaline Phosphatase (ALP) Release. Appl Sci. 2020; 10(11):3840. https://doi.org/10.3390/app10113840.

37. Zhao W, Sachsenmeier K, Zhang L, Sult E, Hollingsworth RE, Yang H. A new Bliss independence model to analyze drug combination data. J Biomol Screen. 2014; 19(5):817–21. https://doi.org/10.1177/1087057114521867 PMID: 24492921.

38. Zheng S, Wang W, Aldahdooh J, Malyutina A, Shadbahr T, Tanoli Z, et al. SynergyFinder Plus: toward better interpretation and annotation of drug combination screening datasets. Genomics Proteomics Bioinformatics. 2022. https://doi.org/10.1016/j.gpb.2022.01.004 PMID: 35085776.

39. Barber AE, Sae-Ong T, Kang K, Seelbinder B, Li J, Walther G, et al. *Aspergillus fumigatus* pan-genome analysis identifies genetic variants associated with human infection. Nat Microbiol. 2021; 6(12):1526–36. https://doi.org/10.1038/s41564-021-00993-x PMID: 34819642.

40. Horta MAC, Steenwyk JL, Mead ME, dos Santos LHB, Zhao S, Gibbons JG, et al. Examination of genome-wide ortholog variation in clinical and environmental isolates of the fungal pathogen *Aspergillus fumigatus*. mBio. 2022; 13(4):e01519–22. https://doi.org/10.1128/mbio.01519-22 PMID: 35766381.

41. Harris BE, Manning BW, Federle TW, Diasio RB. Conversion of 5-fluorocytosine to 5-fluorouracil by human intestinal microflora. Antimicrob Agents Chemother. 1986; 29(1):44–8. https://doi.org/10.1128/AAC.29.1.44 PMID: 3729334.

42. Martinson JNV, Walk ST, Dudley EG. *Escherichia coli* residency in the gut of healthy human adults. EcoSal Plus. 2020; 9(1). https://doi.org/10.1128/ecosalplus.ESP-0003-2020 PMID: 32978935.

43. Ahmad SI, Pritchard RH. Location of the gene specifying cytosine deaminase in *Escherichia coli*. Mol Gen Genet. 1972; 118(4):323–5. https://doi.org/10.1007/BF00333567 PMID: 4570159.

44. Andersen PS, Smith JM, Mygind B. Characterization of the *upp* gene encoding uracil phosphoribosyltransferase of *Escherichia coli* K12. Eur J Biochem. 1992; 204(1):51–6. https://doi.org/10.1111/j.1432-1033.1992.tb16604.x PMID: 1371255.

45. Valentin-Hansen P. Uridine-cytidine kinase from *Escherichia coli*. Methods Enzymol. 1978; 51:308–14. 211379.

46. Pontecorvo G, Roper JA, Hemmons LM, Macdonald KD, Bufton AW. The genetics of *Aspergillus nidulans*. Adv Genet. 1953; 5:141–238. https://doi.org/10.1016/s0065-2660(08)60408-3 PMID: 13040135.

47. Gsaller F, Hortschansky P, Furukawa T, Carr PD, Rash B, Capilla J, et al. Sterol biosynthesis and azole tolerance is governed by the opposing actions of SrbA and the CCAAT binding complex. PLoS Pathog. 2016; 12(7):e1005775. https://doi.org/10.1371/journal.ppat.1005775 PMID: 27438727.

48. Fraczek MG, Bromley M, Buied A, Moore CB, Rajendran R, Rautemaa R, et al. The cdr1B efflux transporter is associated with non-cyp51a-mediated itraconazole resistance in *Aspergillus fumigatus*. J Antimicrob Chemother. 2013; 68(7):1486–96. https://doi.org/10.1093/jac/dkt075 PMID: 23580559.

49. Krappmann S, Jung N, Medic B, Busch S, Prade RA, Braus GH. The *Aspergillus nidulans* F-box protein GrrA links SCF activity to meiosis. Mol Microbiol. 2006; 61(1):76–88. https://doi.org/10.1111/j.1365-2958.2006.05215.x PMID: 16824096.

50. Santos DA, Barros MES, Hamdan JS. Establishing a method of inoculum preparation for susceptibility testing of *Trichophyton rubrum* and *Trichophyton mentagrophytes*. J Clin Microbiol. 2006; 44(1):98–101. https://doi.org/10.1128/JCM.44.1.98-101.2006 PMID: 16390955.

51. Wurster S, Kumaresan PR, Albert ND, Hauser PJ, Lewis RE, Kontoyiannis DP. Live monitoring and analysis of fungal growth, viability, and mycelial morphology using the IncuCyte NeuroTrack processing module. mBio. 2019; 10(3). https://doi.org/10.1128/mBio.00673-19 PMID: 31138745.

52. Meletiadis J, Pournaras S, Roilides E, Walsh TJ. Defining fractional inhibitory concentration index cutoffs for additive interactions based on self-drug additive combinations, Monte Carlo simulation analysis, and *in vitro-in vivo* correlation data for antifungal drug combinations against *Aspergillus fumigatus*. Antimicrob Agents Chemother. 2010; 54(2):602–9. https://doi.org/10.1128/AAC.00999-09 PMID: 19995928.

53. Ubale M, Shioorkar M, Choudhari V. A validated stability-indicating HPLC assay method for flucytosine in bulk drug. Int J Innov Eng Technol. 2017; 8(1):155–61.